PNAS RESEARCH ARTICLE | NEUROSCIENCE OPEN ACCESS

Tmem45b is essential for inflammation- and tissue injury–induced mechanical pain hypersensitivity

Tadashi Tanioku[a], Masayuki Nishibata[a], Yasuyuki Tokinaga[a], Kohtaro Konno[b], Masahiko Watanabe[b], Hiroaki Hemmi[c], Yuri Fukuda-Ohta[c], Tsuneyasu Kaisho[c], Hidemasa Furue[d], and Tomoyuki Kawamata[a,1]

Edited by Tomas Hökfelt, Karolinska Institutet, Stockholm, Sweden; received December 6, 2021; accepted September 11, 2022

Persistent mechanical pain hypersensitivity associated with peripheral inflammation, surgery, trauma, and nerve injury impairs patients' quality of life and daily activity. However, the molecular mechanism and treatment are not yet fully understood. Herein, we show that chemical ablation of isolectin B4-binding ($IB4^+$) afferents by IB4–saporin injection into sciatic nerves completely and selectively inhibited inflammation- and tissue injury–induced mechanical pain hypersensitivity while thermal and mechanical pain hypersensitivities were normal following nerve injury. To determine the molecular mechanism involving the specific types of mechanical pain hypersensitivity, we compared gene expression profiles between $IB4^+$ neuron-ablated and control dorsal root ganglion (DRG) neurons. We identified Tmem45b as one of 12 candidate genes that were specific to somatosensory ganglia and down-regulated by $IB4^+$ neuronal ablation. Indeed, Tmem45b was expressed predominantly in $IB4^+$ DRG neurons, where it was selectively localized in the *trans* Golgi apparatus of DRG neurons but not detectable in the peripheral and central branches of DRG axons. Tmem45b expression was barely detected in the spinal cord and brain. Although Tmem45b-knockout mice showed normal responses to noxious heat and noxious mechanical stimuli under normal conditions, mechanical pain hypersensitivity was selectively impaired after inflammation and tissue incision, reproducing the pain phenotype of $IB4^+$ sensory neuron-ablated mice. Furthermore, acute knockdown by intrathecal injection of Tmem45b small interfering RNA, either before or after inflammation induction, successfully reduced mechanical pain hypersensitivity. Thus, our study demonstrates that Tmem45b is essential for inflammation- and tissue injury–induced mechanical pain hypersensitivity and highlights Tmem45b as a therapeutic target for future treatment.

sensory neuron | pain hypersensitivity | mechanical | pain

Significance

Persistent pain hypersensitivity associated with inflammation, surgery, trauma, and nerve injury interferes with physical and mental activities and impairs quality of life. Herein, we showed that the chemical ablation of isolectin B4-binding ($IB4^+$) afferents suppressed inflammation- and tissue injury–induced mechanical pain hypersensitivity. We identified Tmem45b as a somatosensory-specific molecule that was down-regulated in $IB4^+$-ablated dorsal root ganglia and confirmed its predominant expression in $IB4^+$ primary afferent neurons. Tmem45b-knockout mice showed normal responses to noxious mechanical and noxious thermal stimuli but did not exhibit mechanical pain hypersensitivity in the setting of inflammation and tissue injury. Our findings provide insights into the mechanisms and therapeutic targets for mechanical pain hypersensitivity.

Nociceptive thermal, mechanical, or chemical stimuli excite nociceptors on the peripheral branch of thin myelinated Aδ fiber sensory neurons and unmyelinated C fiber sensory neurons and evoke pain (1, 2). Pain primarily functions as a warning system to alert us to injury and trigger appropriate protective responses (3). Pain is not just a passive consequence of the transfer of peripheral input to the brain but is also an active process (4). Inflammation, tissue injury, or nerve injury can induce pain hypersensitivity characterized by a decreased pain threshold, increased pain intensity, and allodynia, in which a normally innocuous stimulus is perceived as painful (4, 5). Pain hypersensitivity is divided into two main types according to the stimulus modality: thermal and mechanical hypersensitivity. Persistent pain hypersensitivity causes distress to humans beyond the warning signals, interfering with physical and mental activities. Therefore, persistent pain hypersensitivity is an important clinical issue to address (6). Studies using mice deficient in the TRPV1 protein have shown that TRPV1 activation is involved in inflammation- and tissue injury–induced thermal pain hypersensitivity (7, 8), indicating TRPV1 as a potential therapeutic target for thermal pain hypersensitivity. Although several signaling pathways are thought to contribute to the development and maintenance of mechanical pain hypersensitivity (9, 10), the underlying molecular mechanisms remain unexplained (3, 11).

Electrophysiological studies in C-fiber sensory neurons have demonstrated that most nociceptors are polymodal and activated by multiple types of nociceptive stimuli, including thermal and mechanical stimuli (12–14). However, recent studies using the ablation of afferents with specific molecular profiles revealed the existence of distinct subsets of primary sensory neurons that selectively mediate behavioral responses to different noxious stimulus modalities (15). For example, mas-related G-protein coupled receptor (Mrgprd)- and TRPV1-positive primary sensory neurons are selectively required for the perception of noxious mechanical or noxious thermal stimuli, respectively (16). Unmyelinated sensory neurons can be divided into two classes based on their binding to isolectin B4 (IB4) (17, 18). IB4 binding-negative ($IB4^-$) sensory neurons are peptidergic

Author contributions: T. Kawamata designed research; T.T., M.N., Y.T., K.K., and H.F. performed research; M.W., H.H., Y.F.-O., and T. Kaisho contributed new reagents/analytic tools; T.T. and T. Kawamata analyzed data; and M.W., H.F., and T. Kawamata wrote the paper.

The authors declare no competing interest.

This article is a PNAS Direct Submission.

[1]To whom correspondence may be addressed. Email: kawamata@wakayama-med.ac.jp.

This article contains supporting information online at http://www.pnas.org/lookup/suppl/doi:10.1073/pnas.2121989119/-/DCSupplemental.

Published November 2, 2022.

(containing neuropeptides, such as the calcitonin gene-related peptide [CGRP]), and they express tropomyosin receptor kinase A. IB4 binding-positive ($IB4^+$) sensory neurons are nonpeptidergic and express c-Ret neurotrophin and glial cell-derived neurotrophic factor (GDNF) family receptor alpha 1 (19, 20). A genetic ablation study demonstrated that CGRP-positive sensory neurons are involved in heat pain and heat pain hypersensitivity but not mechanical pain in mice (21). This finding highlights the involvement of $IB4^+$ sensory neurons in mechanical pain or mechanical pain hypersensitivity. Chemical ablation of $IB4^+$ sensory neurons by IB4–saporin injection revealed that $IB4^+$ sensory neurons are not involved in normal mechanical and thermal nociception (22) but play a role in GDNF- and carrageenan-induced mechanical pain hypersensitivity (23) and cancer-induced mechanical pain hypersensitivity (24). However, the contribution of $IB4^+$ sensory neurons to other types of pain, such as tissue injury pain and nerve injury pain, remains unknown. In addition, the role of $IB4^+$ sensory neurons in thermal pain hypersensitivity remains unknown. In this study, we first examined the role of $IB4^+$ sensory neurons by evaluating phenotypic changes after neuronal ablation in three pain models. Then, we analyzed the gene expression profiles of $IB4^+$ sensory neurons in the dorsal root ganglion (DRG) to identify molecular candidates and evaluated the role of candidate genes of interest in mechanical pain hypersensitivity using gene knockout (KO) and knockdown (KD) strategies.

Results

Data presented in the *Results* section were obtained from male mice unless otherwise noted.

$IB4^+$ neuronal ablation inhibited inflammation- and tissue injury–induced mechanical pain hypersensitivity. To examine the role of $IB4^+$ sensory neurons in pain sensing, we selectively ablated $IB4^+$ sensory neurons by injecting IB4–saporin into the left sciatic nerve of mice, and an injection of saporin alone was used as the control (25). IB4–saporin injection resulted in the extensive loss of $IB4^+$ terminals but not CGRP-positive terminals in the dorsal horn of the ipsilateral spinal cord (Fig. 1 *A* and *B*). Saporin injection alone did not affect the projections of $IB4^+$ and CGRP-positive terminals. Next, we examined behavioral responses to noxious heat and mechanical stimuli. The ablation of $IB4^+$ sensory neurons had no effect on the latency of paw withdrawal to noxious heat stimuli (thermal test) and the threshold of paw withdrawal to von Frey filaments (mechanical test) compared with the basal level before the injection of IB4–saporin (Fig. 1*C*). This indicates that $IB4^+$ sensory neurons are dispensable for sensing acute noxious thermal and mechanical stimuli under normal conditions, consistent with a previous study (22). We next asked whether $IB4^+$ sensory neurons contribute to pain hypersensitivity in three different pain models: an inflammatory pain model induced by the injection of complete Freund's adjuvant (CFA) into the hind paw, a postoperative pain model induced by surgical tissue incision, and a neuropathic pain model induced by spared nerve injury. In the inflammatory and postoperative pain models, CFA injection or surgical incision decreased the withdrawal latency to noxious heat stimuli (thermal pain hypersensitivity) and the withdrawal threshold to mechanical stimuli with von Frey filaments (mechanical pain hypersensitivity) (Fig. 1 *D* and *E*, black line). In both pain models, mice injected with IB4–saporin exhibited thermal pain hypersensitivity but not mechanical pain hypersensitivity at all time points from 4 to 168 h after CFA injection or surgical incision (Fig. 1 *D* and *E*, green). The neuropathic pain model used in the present study has been reported to show mechanical pain hypersensitivity but not thermal pain hypersensitivity (26). We confirmed this result in saporin-injected control mice and after IB4–saporin injection (Fig. 1*F*), indicating that $IB4^+$ sensory neurons are not involved in mechanical pain hypersensitivity induced in the neuropathic pain model. Taken together, these results show that $IB4^+$ sensory neurons are selectively involved in inflammation- and tissue injury–induced mechanical pain hypersensitivity.

Screening of genes predominantly expressed in $IB4^+$ sensory neurons. To explore molecular candidates mediating mechanical pain hypersensitivity, we used a complementary DNA (cDNA) array to compare gene expression profiles in DRG from mice injected with either IB4–saporin or saporin. We found 43 genes with a >1.5-fold decrease in expression in $IB4^+$ sensory neuron-ablated DRG compared with control DRG, indicating that they are predominantly expressed in $IB4^+$ sensory neurons (Fig. 2*A*). Mishra et al. (2012) detected 153 somatosensory–specific genes by comparing gene expression profiles in two functionally distinct ganglia: the somatosensory trigeminal ganglion and the gustatory geniculate ganglion (27). As an overlap of the two groups, we identified 12 candidate genes that were specific to somatosensory ganglia and predominantly expressed in $IB4^+$ sensory neurons (Fig. 2*B*). Among these candidates, we selected *Tmem45b* for further analysis because its function and expression in the nervous system remain unknown and it was predominantly expressed in $IB4^+$ sensory DRG neurons, as shown in the section below.

Tmem45b is predominantly expressed in $IB4^+$ sensory neurons. Next, we examined the tissue expression of Tmem45b mRNA by qRT-PCR analysis. Tmem45b messenger RNA (mRNA) was highly expressed in the aorta, urinary bladder, and digestive tracts (Fig. 3*A*). Intriguingly, within the nervous system, Tmem45b mRNA was exclusively detected in DRG, with low or no detectable expression in the spinal cord and brain. Double staining by in situ hybridization and IB4 lectin binding revealed that most $IB4^+$ sensory neurons in DRG (91.8 ± 1.8%, $n = 4$ mice) expressed Tmem45b mRNA (Fig. 3*B*). Next, we examined Tmem45b protein expression in DRG by producing a rabbit polyclonal antibody and validating its specificity by comparing immunohistochemical and immunoblot labeling between wild-type (WT) and Tmem45b-KO DRG and by confirming colabeling with Tmem45b mRNA in WT DRG (*SI Appendix*, Fig. S1). Immunohistochemical analysis showed that Tmem45b-positive neurons accounted for 38 ± 1.5% of total DRG neurons and that Tmem45b was selectively expressed in small-sized DRG neurons (somal area, < 600 μm^2) but was rarely expressed in medium- to large-sized DRG neurons (Fig. 3 *C* and *D*). Tmem45b was localized selectively in the *trans* Golgi apparatus on the basis of immunofluorescence and immunoelectron microscopic data (Fig. 3E). To characterize the neurochemical profile of Tmem45b-positive DRG neurons, double immunostaining with several neuronal subset markers was performed, including TRPV1 (noxious heat-sensitive sensory neurons), IB4 (nonpeptidergic sensory neurons), CGRP (peptidergic sensory neurons), and NF200 (myelinated sensory neurons). Tmem45b was expressed in most (93.5 ± 2.4%) $IB4^+$ sensory neurons but only a small proportion of other neuronal populations: 19.1 ± 1.1% of TRPV1-positive sensory neurons, 7.1 ± 1.3% of CGRP-positive sensory neurons, and 0.1 ± 0.1% of NF200-positive sensory neurons (Fig. 3*F* and *SI Appendix*, Table S1). Consistent with the results of the double immunostaining experiment, the ablation of $IB4^+$ sensory neurons using IB4–saporin greatly

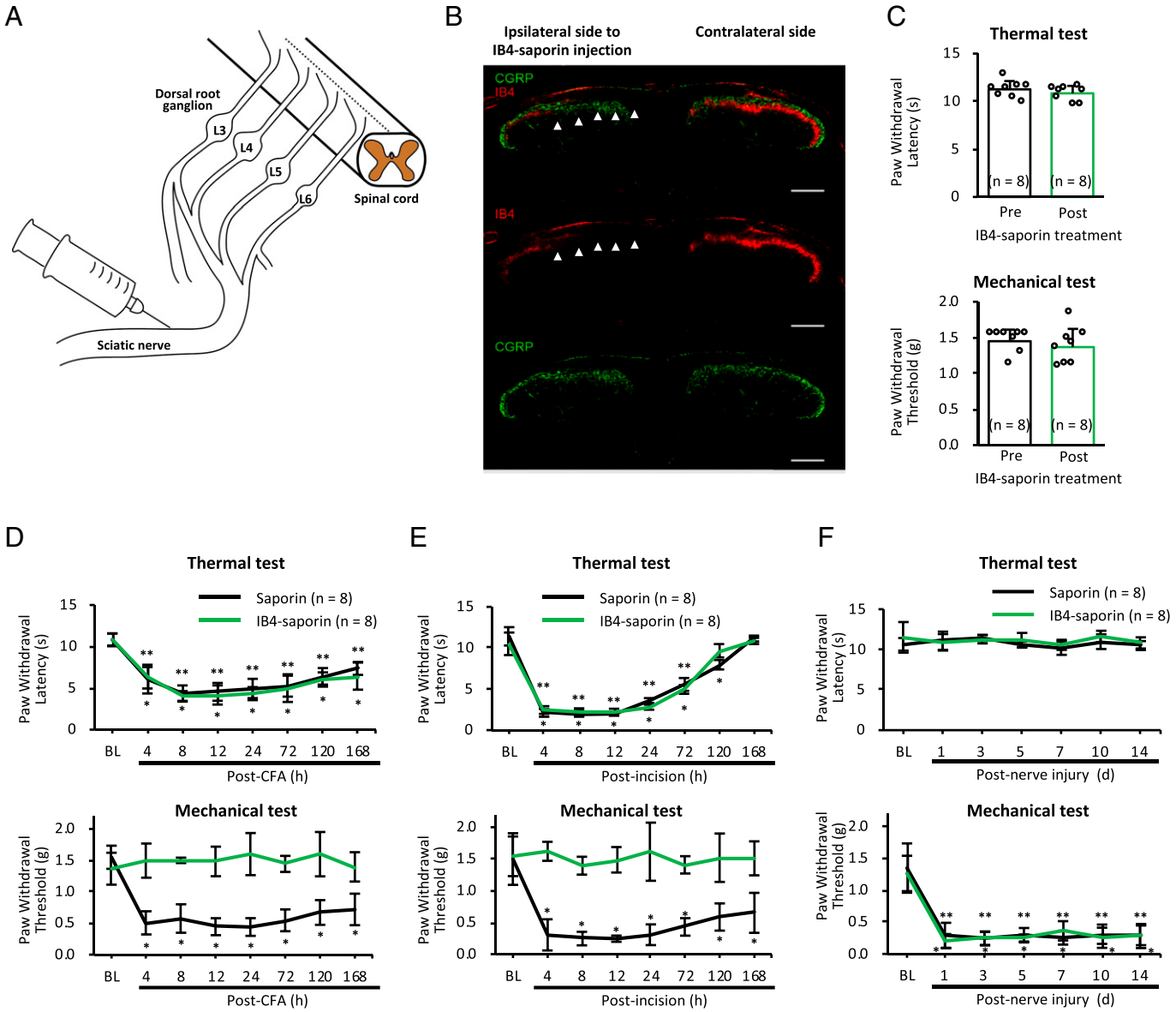

Fig. 1. IB4-binding neurons are critical for inflammation- and tissue injury–induced mechanical pain hypersensitivity. (*A*) Schematic of IB4–saporin or saporin injection into the left sciatic nerve. (*B*) IB4–saporin selectively ablated IB4$^+$ afferents (red) but not CGRP-positive afferents (green) in the dorsal horn of the spinal cord on the ipsilateral side to IB4–saporin injection. Immunostaining was performed 7 d after IB4–saporin injection. White arrowheads indicate the elimination of IB4$^+$ afferents (Scale bar, 200 μm). (*C*) Ablation of IB4$^+$ neurons had no effect on the withdrawal latency to noxious heat stimuli (thermal test, *Top*) or withdrawal threshold to von Frey filaments (mechanical test, *Bottom*) before IB4–saporin injection vs. 7 d after IB4–saporin injection, $P = 0.45$ for withdrawal latency, $P = 0.62$ for withdrawal threshold; 2-tailed paired Student's *t* test. (*D*–*F*) Effects of IB4–saporin treatment in three different pain models: (*D*) CFA-induced inflammation pain model, (*E*) Incision-induced tissue injury pain model, (*F*) Peripheral nerve injury–induced neuropathic pain model. IB4–saporin treatment selectively inhibited mechanical pain hypersensitivity in the inflammation pain model (*D*) and tissue injury pain model (*E*). In each figure, the upper panel shows the time courses of withdrawal latency to noxious heat stimuli, and the lower panel shows the withdrawal threshold to von Frey filaments. BL = basal level the value before CFA injection, tissue incision, or nerve injury. Mice receiving saporin (black) and mice receiving IB4–saporin (green) in each pain model, *$P < 0.0001$ vs. BL within a group comparison of mice receiving saporin, **$P < 0.0001$ vs. BL within a group comparison of mice receiving IB4–saporin; 1-way ANOVA followed by Dunnett's test. All data are presented as mean ± SD.

decreased the number of Tmem45b-positive neurons (*SI Appendix*, Fig. S2).

Next, we examined expression and projection in the central and peripheral axon branches of Tmem45b-positive DRG neurons. In the spinal cord, peptidergic sensory neurons are known to project predominantly to lamina I and the outer lamina II, whereas nonpeptidergic sensory neurons terminate in the inner lamina II (28). Consistently, IB4$^+$ central afferents terminated in the inner lamina II, where weak noise labeling to Tmeme45b was discerned in both WT and Temem45b-KO mice (Fig. 3*G*). This indicates that the IB4$^+$ central branch normally projected from Tmem45b-KO DRG neurons to the dorsal horn, but no specific signals for Tmem45b were detectable in the central branch. Likewise, we could not find Tmem45b-positive peripheral branch in the glabrous skin.

Next, to examine the peripheral projection of Tmem45b-expressing sensory neurons, we injected the retrograde neuronal tracer Fast Blue (FB) into peripheral tissues and organs and examined the extent of FB and Tmem45b colabeling at the corresponding level of DRG (Fig. 3*H*). Following FB injection into the glabrous skin, we found that 28.1 ± 1.5% and 35.9 ± 4.2% of FB-labeled DRG neurons expressed Tmem45b in the hind paw or the tibialis anterior muscle, respectively. In contrast, the percentage was considerably lower after FB injection into the

A

Fold Change	Gene Symbol	Acc number	Fold Change	Gene Symbol	Acc number
-2.24	Mrgprx1	NM_207540	-1.62	A3galt2	NM_001009819
-2.21	Mrgprb5	NM_207538	-1.60	Trpa1	NM_177781
-2.09	Mrgpra3	NM_153067	-1.59	Kcnt1	NM_175462
-2.05	Chrna6	NM_021369	-1.59	Dgki	NM_001081206
-1.93	Mrgprd	NM_203490	-1.58	Gpr165	NM_029536
-1.77	Gm16364	NR_152259	-1.57	Tmem45b	NM_144936
-1.75	Ctxn3	NM_001134697	-1.57	Kcnmb1	NM_031169
-1.75	Syt10	NM_018803	-1.57	Moxd1	NM_021509
-1.73	Rasgrp1	NM_011246	-1.56	Ano3	NM_001128103
-1.72	Hs6st2	NM_001077202	-1.55	D130009I18Rik	NR_015593
-1.71	Gm7271	NR_033501	-1.55	Gm16532	NM_001134752
-1.70	Lpar3	NM_022983	-1.54	Fam188b2-ps	NM_001142781
-1.70	Kcng3	NM_153512	-1.54	Pld5	NM_176916
-1.68	Ldb2	NM_010698	-1.54	Grik1	NM_146072
-1.66	Scn11a	NM_011887	-1.53	Paqr5	NM_028748
-1.66	Cd55	NM_010016	-1.53	Tmem255a	NM_172930
-1.65	Trpc3	NM_019510	-1.52	Prkcq	NM_008859
-1.65	Ica1l	NM_001357296	-1.52	Olfr1000	NM_001011695
-1.65	Gm21889; Gm21920		-1.51	Prkar2b	NM_011158
-1.64	Mal2	NM_178920	-1.50	Gna14	NM_008137
-1.63	Cyp4f39	NM_177307	-1.50	Slc35f4	NM_029238
-1.62	St6gal2	NM_001347403			

B

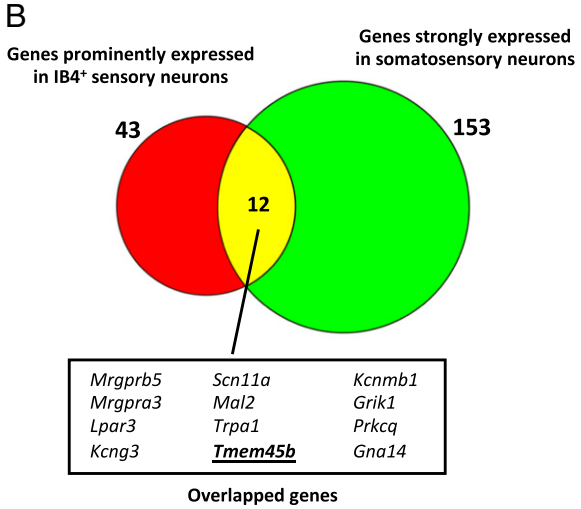

Fig. 2. Identification of Tmem45b. (*A*) List of 43 genes differentially expressed between IB4$^+$ neuron-ablated (IB4–saporin injection) and control (saporin injection) DRG. Genes with a > 1.5-fold decrease in IB4$^+$ neuron-ablated DRG were selected as predominantly differentially expressed genes ($n = 3$). (*B*) Schematic of the selection of genes of interest. Red and green circles indicate 43 genes prominently expressed in IB4$^+$ neurons and 153 genes selectively expressed in somatosensory ganglia shown by Mishra et al., respectively (27). The yellow region indicates 12 overlapped genes that are somatosensory–specific and predominantly expressed in IB4$^+$ neurons.

urinary bladder (3.2 ± 1.8%) and distal colon (1.2 ± 1.2%) (Fig. 3*H* and *SI Appendix*, Table S2). These histochemical findings indicate that Tmem45b is predominantly expressed in IB4$^+$ sensory neurons and selectively localized in the *trans* Golgi. Moreover, Tmem45b-positive DRG neurons preferentially innervate the skin and skeletal muscle rather than visceral organs.

No significant sex differences were noted in the percentage of Tmem45b-positive neurons among DRG neurons (38.1 ± 1.5% in males vs. 38.6 ± 4.3% in females), neurochemical profiles of Tmem45b-positive DRG neurons (*SI Appendix*, Table S1 for males and *SI Appendix*, Table S3 for females), and cell-size distribution of Tmem45b-positive cells in DRG neurons (Fig. 3*D* for males and *SI Appendix*, Fig. S3 for females). To further examine whether peripheral inflammation affects the predominant expression of Tmem45b in IB4$^+$ neurons, we counted the percentages of IB4$^+$ and IB4$^-$ neurons in Tmem45b-positive DRG neurons and found no significant difference between naïve mice and CFA-injected mice (*SI Appendix*, Fig. S4).

Tmem45b is essential for inflammation- and tissue injury–induced mechanical pain hypersensitivity. To clarify the role of Tmem45b in pain sensing, we produced Tmem45b-KO mice (Fig. 4*A* and *SI Appendix*, Fig. S5). Tmem45b-KO mice were viable and did not show any overt motor defects or reflex impairments. Gait and locomotion in Tmem45b-KO mice were similar to those in WT mice (*SI Appendix*, Fig. S6). The withdrawal latency to noxious heat stimuli and the withdrawal threshold to von Frey filaments in Tmem45b-KO mice were comparable to those in WT mice (Fig. 4*B*), indicating that Tmem45b is not involved in behavioral responses to acute noxious heat and noxious mechanical stimuli under normal conditions. In addition, neither WT mice nor Tmem45b-KO mice showed any spontaneous pain-related behaviors under normal conditions. We next examined the contribution of Tmem45b to pain hypersensitivity in a CFA-induced inflammatory pain model. In both WT and Tmem45b-KO mice, CFA injection into the hind paw comparably induced paw edema (*SI Appendix*, Fig. S7) and long-lasting thermal pain hypersensitivity (Fig. 4*C*, *Top*). However, long-lasting mechanical pain hypersensitivity was induced in WT mice but not Tmem45b-KO mice at all time points during the observation period (Fig. 4*C*, *Bottom*). A similar selective loss of mechanical pain hypersensitivity was observed for Tmem45b-KO mice following surgical tissue incision (Fig. 4*D*) but not following spared nerve injury (Fig. 4*E*). These findings highlight the involvement of Tmem45b in specific types of mechanical pain hypersensitivity, including inflammation- and tissue injury–induced hypersensitivity. Finally, to examine sex differences in pain-related behaviors, we tested WT and Tmem45b-KO female mice in the same behavioral experiments and found no significant sex differences (Fig. 4 *B*–*E* for males and *SI Appendix*, Fig. S8 for females).

Acute Tmem45b KD also inhibits mechanical pain hypersensitivity. To exclude the possibility of secondary developmental influences of gene KO on behavioral responses, rather than a direct effect of the loss of Tmem45b function, we examined the effects of acute KD by small interfering RNA (siRNA). Using Lewis lung carcinoma cells, which constitutively express Tmem45b, we confirmed that siRNA knocked down the expression of Tmem45b mRNA to ∼20% compared with scrambled siRNA (*SI Appendix*, Fig. S9). Tmem45b siRNA or scrambled siRNA was intrathecally administered once a day for 3 consecutive days before (pretreatment) or after (posttreatment) CFA injection into the hind paw (Fig. 5*A*). In the pretreatment experiment, intrathecal injection of Tmem45b siRNA or scrambled siRNA did not change the withdrawal threshold to von Frey filaments compared with the threshold before intrathecal injection (Fig. 5*A*, *Top*). Then, CFA was injected 24 h after the third intrathecal injection. Of note, mechanical pain hypersensitivity was significantly reduced in mice injected with Tmem45b siRNA compared with scrambled siRNA (Fig. 5*A*, *Top*). For the posttreatment experiment in which CFA injection preceded intrathecal siRNA injection, the injection of Tmem45b siRNA partially but significantly reversed mechanical pain hypersensitivity compared with the injection of scrambled siRNA (48 h after the third siRNA administration). In both treatment experiments, intrathecal injection of Tmem45b siRNA significantly reduced Tmem45b mRNA levels in DRG compared with scrambled siRNA (Fig. 5*B*). The similar phenotypes between Tmem45b-KO and Tmem45b-KD mice support the suggestion that the behavioral loss of mechanical pain hypersensitivity is likely caused by the loss of Tmem45b function. Furthermore, the preventive

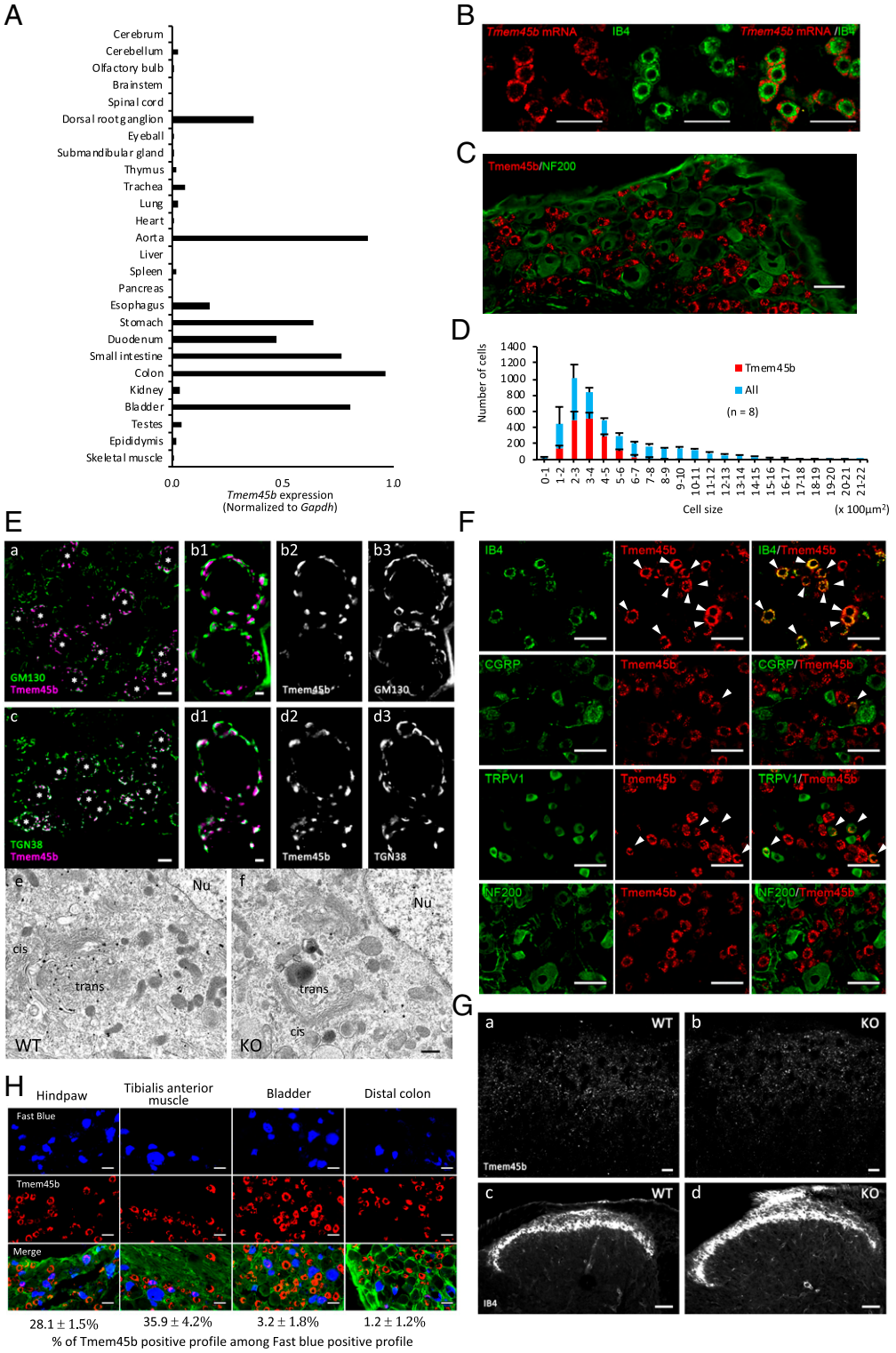

Fig. 3. Tissue- and neuron type–specific expression of Tmem45b. (*A*) qRT-PCR analysis. Tmem45b is highly transcribed in the DRG, aorta, urinary bladder, and digestive tracts in mouse tissues. Bars represent Tmem45b mRNA expression normalized to Gapdh. (*B*) Expression of Tmem45b mRNA (fluorescent in situ hybridization, red) in IB4$^+$ (green) DRG neurons (Scale bar, 50 μm). (*C*) Immunofluorescence for Tmem45b (red) and NF200 (green), a marker of myelinated neurons in DRG (Scale bar, 50 μm). (*D*) Cell size distribution of Tmem45b-positive cells in L4/5 DRG; $n = 8$ mice. (*E*) Localization of Tmem45b in the *trans* Golgi. *a–d*, Immunofluorescence shows good overlap with *trans*-Golgi marker TGN38 (*Middle*) and side-by-side apposition to *cis*-Golgi marker GM130 (*Top*). Asterisks indicate Tmem45b-positive neurons. *e–f*, Silver-enhanced immunogold electron microscopy shows metal particle labeling in the *trans* Golgi apparatus in WT but not Tmem45b-KO, DRG. Nu = nucleus (Scale bar, 10 μm in *a* and *c*; 2 μm in *b1–3* and *d1–3*; 400 nm in *e* and *f*). (*F*) Double immunofluorescence for Tmem45b (red) and several neuronal subset markers (green), including IB4 (nonpeptidergic unmyelinated neuron), CGRP (peptidergic neuron), TRPV1 (heat- and capsaicin-sensitive nociceptive neuron), and NF200 in DRG. Arrowheads indicate double positive neurons; $n = 4$ mice (Scale bars, 50 μm). (*G*) Lack of specific signals for Tmem45b in IB4$^+$-projecting regions in the spinal dorsal horn (*a* and *b*, immunofluorescence for Tmem45b; *c* and *d*, immunofluorescence for IB4) (Scale bars, 10 μm in *a* and *b*; 50 μm in *c* and *d*). (*H*) Differential projection of Tmem45b-positive DRG neurons to peripheral tissues and organs. Fast Blue (FB; blue) was injected into the glabrous skin in the hind paw, tibialis anterior muscle, urinary bladder, and distal colon, and DRG sections were immunostained for Tmem45b (red) and the neuronal marker PGP9.5 (green). The percentage of Tmem45b/FB-double positive neurons among total FB-labeled neurons is indicated at the bottom (Scale bar, 50 μm). All data are presented as mean ± SD.

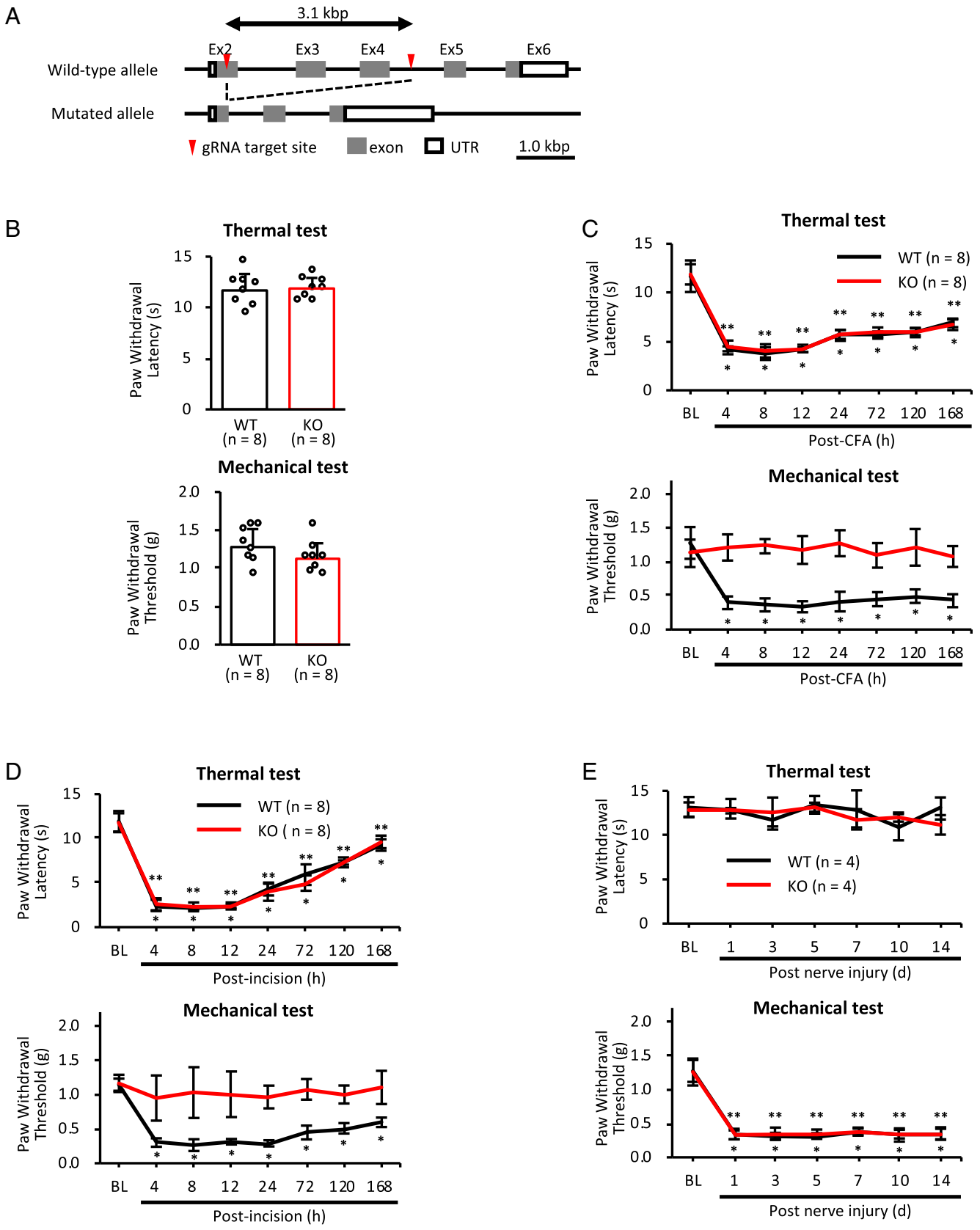

Fig. 4. Tmem45b KO inhibits inflammation- and tissue injury–induced mechanical pain hypersensitivity. (*A*) Generation of Tmem45b-KO mice. Targeting mediated by two gRNAs induces deletion of a 3.1 kbp gene fragment as indicated by red arrowheads. UTR, untranslated region. (*B*) Tmem45b KO does not affect the withdrawal latency to noxious heat stimuli (thermal test, *Top*, $P = 0.91$) or withdrawal threshold to von Frey filaments (mechanical test, *Bottom*, $n = 8$, $P = 0.39$); 2-tailed unpaired Student's t test. (*C*–*E*) Effects of Tmem45b KO on pain hypersensitivity in three different pain models: (*C*) CFA-induced inflammation pain model, (*D*) Incision-induced tissue injury pain model, (*E*) Peripheral nerve injury–induced neuropathic pain model. Tmem45b KO selectively inhibited mechanical pain hypersensitivity in the inflammation pain model (*C*) and tissue injury pain model (*D*). *$P < 0.0001$ vs. BL within a group comparison of WT mice, **$P < 0.0001$ vs. BL within a group comparison of the KO mice; 1-way ANOVA followed by Dunnett's test. All data are presented as mean ± SD. BL corresponds to the value before CFA injection, tissue incision, or nerve injury.

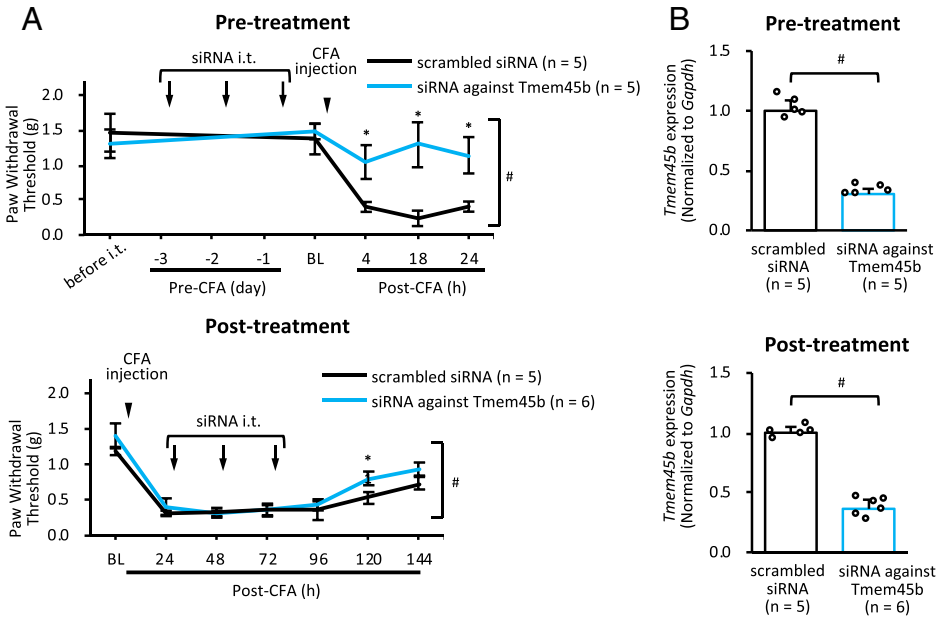

Fig. 5. Effects of siRNA-mediated Tmem45b KD on mechanical pain hypersensitivity. (*A*) Effects of siRNA KD of Tmem45b on mechanical pain hypersensitivity in the CFA-induced inflammation pain model. siRNA against Tmem45b (blue) or scrambled siRNA (black) was administered for 3 consecutive days before CFA injection (pretreatment) or after CFA injection (posttreatment). For pretreatment, $^{\#}P < 0.0001$, siRNA against Tmem45b vs. scrambled siRNA, 2-way ANOVA; $^{*}P < 0.0002$ between group comparisons at each time point; 2-tailed unpaired Student's *t* test for the analysis of pretreatment. For posttreatment, $^{\#}P < 0.004$, siRNA vs. scrambled siRNA, 2-way ANOVA; $^{*}P < 0.0002$ between group comparisons at each time point; 2-tailed unpaired Student's *t* test for the analysis of posttreatment. Before i.t. refers to a value before siRNA injection. (*B*) Effects of siRNA on Tmem45b mRNA levels in DRG. L4/5/6 DRG neurons were sampled after the last behavioral assessment in both cases. Columns show the mean expression level of Tmem45b mRNA normalized to *Gapdh*. Numbers of mice analyzed are indicated at the bottom of each column. $^{\#}P < 0.0001$, siRNA against Tmem45b vs. scrambled siRNA; 2-tailed unpaired Student's *t* test. All data are presented as mean ± SD. BL corresponds to the value before CFA injection.

effect of siRNA injection on mechanical pain hypersensitivity highlights the potential of Tmem45b as a target for future treatment of mechanical pain hypersensitivity.

Decrease in C-fiber inputs to substantia gelatinosa neurons in Tmem45b-KO mice in a CFA-induced inflammatory pain model. Finally, to examine the effects of Tmem45b KO on spinal synaptic transmission, we compared synaptic responses evoked in substantia gelatinosa (SG) neurons in the spinal cord of CFA-injected WT (WT-CFA) and Tmem45b-KO mice (KO-CFA). Regarding spontaneous excitatory postsynaptic currents (EPSCs) recorded from SG neurons, no significant differences were found in the frequency (WT-CFA, 3.9 ± 0.8 Hz, $n = 10$; KO-CFA, 4.3 ± 0.9 Hz, $n = 10$; $P = 0.72$) or amplitude (WT-CFA, 10.7 ± 1.2 pA, $n = 10$; KO-CFA, 12.1 ± 0.8 pA, $n = 10$; $P = 0.28$). Dorsal root stimulation elicited monosynaptic and polysynaptic EPSCs in SG neurons in both mice (Fig. 6*A*). In total, 11 monosynaptic C-fiber–mediated and nine monosynaptic A-fiber–mediated EPSCs were detected from 11 SG neurons in WT-CFA mice, and three monosynaptic C-fiber– and nine monosynaptic A-fiber–mediated EPSCs were from 11 SG neurons in KO-CFA mice. There were no differences in the mean amplitudes of monosynaptic C-fiber– and A-fiber–mediated EPSCs between the two mice (Fig. 6*B*). In WT-CFA mice, we detected C-fiber–mediated EPSCs with various stimulus intensities (Fig. 6*C*, *Left*). However, such multiple synaptic inputs were rarely detected in KO-CFA mice (Fig. 6*C*, *Right*). In composition analysis, multiple (≥ 2), single, and no C-fiber–mediated EPSCs were recorded in four, five, and two SG neurons, respectively, from WT-CFA mice, and in one, eight, and 13 SG neurons, respectively, from KO-CFA mice, showing a significant genotypic difference for C-fiber–mediated EPSCs (Fig. 6*D*). The ratio of IB4^{+} DRG neurons (mostly Tmem45b positive) to NF200-positive DRG neurons (mostly Tmem45b negative) was comparable between WT-CFA (0.97 ± 0.05, $n = 3$) and KO CFA mice (0.96 ± 0.11, $n = 3$) ($P = 0.91$). (Fig. 6*E*). These findings suggest that the number of C-fiber–excitatory synaptic inputs to single SG neurons was decreased in KO-CFA mice, which was unlikely due to IB4^{+} neuron loss.

Discussion

In this study, we demonstrated that Tmem45b is not involved in sensing noxious stimuli under normal conditions but is essential for inflammation- and tissue injury–induced mechanical pain hypersensitivity. Because neurochemical characteristics of IB4^{+} sensory neurons appear to be more heterogeneous in rats than in mice (29), behavioral phenotypes after the ablation of IB4^{+} sensory neurons may not be identical between these two species. For example, the ablation of IB4^{+} sensory neurons affects thermal nociception in rats (30) but not in mice (22). Therefore, we discuss our present results by mainly citing data from mouse experiments, unless otherwise noted.

Involvement of IB4^{+} sensory neurons in inflammation- and tissue injury–induced mechanical pain hypersensitivity. In this study, we confirmed the previous finding that IB4^{+} sensory neurons did not contribute to behavioral responses to noxious thermal and noxious mechanical stimuli under normal conditions (22, 23). We further determined that IB4^{+} sensory neurons were not involved in inflammation- and tissue incision–induced thermal pain hypersensitivity. The lack of functional involvement of IB4^{+} sensory neurons in behavioral responses to noxious thermal stimuli and thermal pain hypersensitivity may be explained by the fact that only a small percentage (2–5%) of IB4^{+} sensory neurons express TRPV1 (31–33). Regarding the fact that IB4^{+} sensory neurons were dispensable for sensing noxious mechanical stimuli under normal conditions, it should

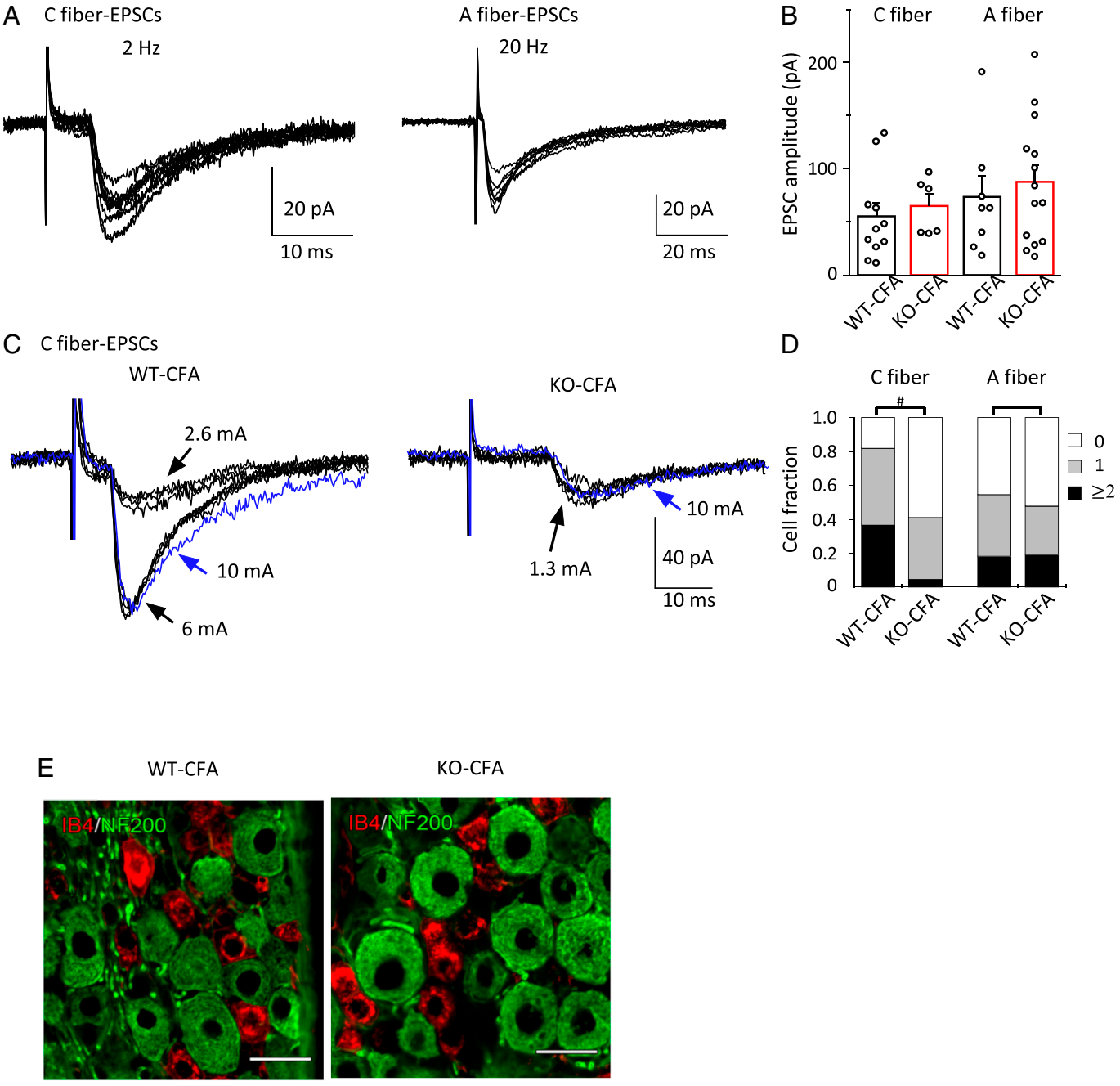

Fig. 6. Afferent-evoked spinal synaptic responses in CFA-injected WT and Tmem45b-KO mice. (*A*) Representative monosynaptic A- and C-fiber–mediated EPSCs evoked in SG neurons of WT mice by dorsal root repetitive stimulation. (*B*) Summary graph showing the amplitudes of monosynaptic C- and A-fiber–mediated EPSCs in CFA-injected WT-CFA and Tmem45b-KO-CFA mice (C-fiber, $P = 0.61$; A-fiber, $P = 0.58$, unpaired t test). (*C*) Representative traces showing C-fiber EPSCs evoked in SG neurons in WT-CFA and Tmem45b-KO-CFA mice. When stimulus intensity was gradually increased at 0.2 Hz up to a maximum stimulus intensity of 10 mA, C-fiber EPSCs with different stimulus thresholds of 2.6 and 6 mA were evoked in WT-CFA mice, indicating that the recorded neuron had received synaptic inputs from two C-fibers with different stimulus thresholds. In Tmem45b-KO-CFA mice, C-fiber EPSCs with a threshold of 1.3 mA were elicited. Traces (blue color) recorded at a stimulus intensity of 10 mA were superimposed. (*D*) Stacked histograms showing composition of C-fiber and A-fiber EPSC numbers detected in single SG neurons of WT-CFA and Tmem45b-KO-CFA mice (C-fiber, $^{\#}P = 0.02$; A-fiber, $P = 0.89$; chi-square test); 0, no input; 1, one input; ≥ 2, 2 or more inputs. (*E*) Double immunofluorescence for Tmem45b (red) and NF200 (green) in DRG in WT-CFA and Tmem45b-KO-CFA mice.

be noted that the ablation of Mrgprd-positive neurons, which are included in IB4$^+$ sensory neurons (34), reduces behavioral sensitivity to noxious mechanical stimuli and inhibits inflammation-induced mechanical pain hypersensitivity (16). Because IB4$^+$ sensory neurons were not completely eliminated in the present and previous studies using IB4–saporin (22, 23), a small number of viable IB4$^+$ sensory neurons could mediate noxious mechanical sensation. It should also be noted that following the ablation of voltage-gated sodium channel Nav1.8-positive sensory neurons, which include > 85% of nociceptive neurons and all IB4$^+$ sensory neurons, withdrawal responses to von Frey filaments are normally preserved, but those responses to high threshold mechanical forces are impaired (35). Therefore, behavioral responses to noxious mechanical stimuli may vary depending on experimental procedures and the nature of mechanical stimuli, and the role of IB4$^+$ sensory neurons in noxious mechanical sensation needs to be further pursued in future studies.

Together, the present and previous studies clarified that IB4$^+$ sensory neurons are involved in mechanical pain hypersensitivity in various pain models, including CFA-, tissue incision–, carrageenan-, GDNF-, or cancer-induced nociceptive pain models (22, 23). However, the ablation of IB4$^+$ sensory neurons did not abolish mechanical pain hypersensitivity in the neuropathic pain model induced by spared peripheral nerve injury. This finding is consistent with experiments using rats in which the ablation of IB4$^+$ sensory neurons did not inhibit mechanical pain hypersensitivity induced by chronic constriction of the mental nerve (36). In addition, CGRP-positive sensory neurons do not contribute to mechanical pain hypersensitivity induced by peripheral nerve injury (21). Overall, it is likely that different neuronal populations are involved in mechanical pain hypersensitivity induced in different pain models, such as IB4$^+$ sensory neurons in nociceptive pain models and IB4$^-$ sensory neurons, presumably thin myelinated nociceptors, in neuropathic pain models.

Tmem45b is predominantly expressed in IB4$^+$ sensory neurons. We searched for candidate molecules involved in mechanical pain hypersensitivity. To this end, we compared gene expression profiles between IB4$^+$ sensory neuron-ablated DRG and control DRG. Tmem45b was identified as one of 12 somatosensory–specific genes that were down-regulated in IB4$^+$ sensory neuron-ablated DRG. Within the nervous system, Tmem45b was expressed almost selectively in DRG, where it was predominantly expressed in IB4$^+$ sensory neurons (91.8% of IB4$^+$ sensory neurons). In addition, 19.1% of TRPV1-positive sensory neurons expressed Tmem45b. Given that only 2 to 5% of TRPV1-positive sensory neurons are IB4$^+$ (32, 33), the majority of Tmem45b-expressing TRPV1-positive neurons may be IB4$^-$. In contrast, low Tmem45b expression rates were detected in CGRP-positive (7.1%) and NF200-positive (0.1%) sensory neurons. These neurochemical expression profiles are consistent with single-cell RNA sequencing and microarray studies in which Tmem45b was mainly expressed in nonpeptidergic, small- to medium-sized DRG neurons (37–39). Tmem45b was highly expressed in some peripheral organs, including the aorta, urinary bladder, and digestive tracts. Intriguingly, all of these peripheral organs change their size and form in response to mechanical stimuli. Therefore, the cellular expression and function of Tmem45b should be addressed in these organs.

Involvement of Tmem45b in inflammation- and tissue injury–induced mechanical pain hypersensitivity. The role of Tmem45b in noxious mechanical sensing and mechanical pain hypersensitivity was tested by analyzing behavioral responses in Tmem45b-KO and WT mice. To our surprise, pain-related behavioral phenotypes in Tmem45b-KO mice were identical to those in IB4$^+$ sensory neuron-ablated mice (i.e., selective abolishment of inflammation- and tissue injury–induced mechanical pain hypersensitivity). This common phenotype, together with the notion that most Tmem45b-expressing TRPV1-positive neurons are IB4$^-$, suggests that Tmem45b in IB4$^+$ sensory neurons is responsible for mechanical pain hypersensitivity in nociceptive pain models. In this study, the CFA-induced inflammation pain model and skin incision–induced tissue injury pain model were used as nociceptive pain models. These two pain models exhibit similar long-lasting mechanical pain hypersensitivity (40), but the spinal mechanisms of pain hypersensitivity are different between the two models (40, 41). Our study indicates that Tmem45b is involved in a common peripheral mechanism of inflammation- and tissue injury–induced mechanical pain hypersensitivity. In addition, Tmem45b did not contribute to behavioral responses to noxious thermal and noxious mechanical stimuli under normal conditions. An ablation study has indicated that Tmem45b-positive afferents are not involved in noxious withdrawal responses to punctate mechanical stimuli using von Frey filaments under normal conditions, but they are involved in withdrawal responses to pressure mechanical stimuli in the Randall Selitto test (42). Tmem45b may also be involved in sensing pressure mechanical stimuli.

Tmem45b immunoreactivity was selectively localized in the *trans* Golgi of DRG neurons, but not in their axons. Moreover, we determined that Tmem45b-expressing DRG neurons preferentially innervated the skin and skeletal muscle rather than visceral organs. The absence of Tmem45b in the central and peripheral branches of primary sensory afferents suggests that Tmem45b by itself acts neither as a transducer to the spinal cord nor as a mechanical sensor in the skin and skeletal muscle. According to an in silico study, Tmem45b is a 7-transmembrane (TM) protein (43) but does not have typical G-protein–coupled receptor amino acid sequence motifs, such as the CWxP motif in TM6, the NPxxY motif in TM7, or the D/ERY motif in TM3 (44). Although Tmem45b has been reported to be involved in the development of several types of cancer (45–48), its functions and mechanisms in inflammation- and tissue injury–induced mechanical pain hypersensitivity remain completely unknown. A recent single-neuron transcript study has shown that the C low threshold mechanoreceptor, which contributes to mechanical pain hypersensitivity (49), expresses Tmem45b (50). On the basis of the selective intracellular localization in the *trans* Golgi and the decrease in the number of C-fiber inputs to SG neurons, Tmem45b may contribute to maturating, sorting, and transporting vital molecules involved in, for example, action potential generation or neurotransmitter release in C-fibers responsible for mechanical pain hypersensitivity. Such a chaperon-like function for the modulation and assembly of ion channels and receptors has been shown for Tmem163 and Tmem35 (51, 52). It has been reported that somatostatin-positive spinal interneurons are indispensable for the reduction of withdrawal thresholds to von Frey filaments following persistent inflammation (53). Therefore, Tmem45b-positive afferents may mono- or polysynaptically connect with somatostatin-positive interneurons in the spinal cord, resulting in mechanical pain hypersensitivity.

Tmem45b as a potential therapeutic target for mechanical pain hypersensitivity. KD experiments using siRNA showed that both pre- and posttreatment with siRNA against Tmem45b reduced mechanical pain hypersensitivity induced by CFA injection, highlighting the involvement of Tmem45b in the development and maintenance of inflammation-induced mechanical pain hypersensitivity. Furthermore, the greater inhibitory effects of pretreatment compared with posttreatment favors the important role of Tmem45b in the developmental phase of mechanical pain hypersensitivity. Our KO and KD experiments collectively suggest that Tmem45b provides a potential therapeutic target for inflammatory- and tissue injury–induced mechanical pain hypersensitivity for two reasons. First, Tmem45b KD did not affect the sensitivity to physiological pain, a warning signal that triggers appropriate protective responses. Second, Tmem45b was mainly expressed in peripheral sensory neurons but not central neurons. Therefore, this therapeutic approach is expected to reduce pathologic pain while avoiding possible side effects involving the central nervous system, such as addiction. In opioid therapy,

addiction is known to cause serious health concerns, which has led to the so-called opioid crisis (54).

In conclusion, our study demonstrates that Tmem45b is mainly expressed in $IB4^+$ sensory neurons and plays an essential role in the induction and maintenance of mechanical pain hypersensitivity in nociceptive pain models. These findings provide insights into the mechanisms and future treatment for persistent mechanical pain hypersensitivity.

Materials and Methods

All experimental procedures were approved by the Wakayama Medical University Animal Care and Use Committee (Wakayama, Japan) and performed in accordance with the ethical guidelines of the NIH and of the International Association for the Study of Pain. Detailed descriptions of methods and materials are provided in SI Appendix, Materials and Methods.

Animals. Adult male and female C57BL/6N mice and Tmem45b-KO C57BL/6N mice were used for experiments. The mice were housed in a temperature-controlled (21 ± 1 °C) room under a 12 h light/dark cycle and given food and water ad libitum.

Deletion of IB4-binding afferents in sciatic nerves. To examine the role of IB4-binding afferents, IB4–saporin (Advanced Targeting Systems) was injected into the left sciatic nerve. Animals without any motor impairment were used for experiments 7–10 d after injection. After behavioral tests, the deletion of $IB4^+$ afferents was evaluated by the loss of IB4 binding in the dorsal horn of the L4–L5 spinal cord.

Generation of Tmem45b-KO mice. Tmem45b-KO mice were generated by clustered regularly interspaced short palindromic repeats (CRISPR)/CRISPR-associated protein 9 (Cas9)-mediated genome editing. Single cell–stage fertilized embryos from B6C3F1 females mated with C57BL/6N males were injected with guide RNAs and Cas9 mRNA and transferred to the oviducts of pseudopregnant foster mice. Founders bearing *Tmem45b* deletion were identified by PCR.

In vivo KD of Tmem45b. The sense and antisense siRNA sequences were 5′-CUUAUGUGCUCCUAGGGCU-3′ and 5′-AGCCCUAGGACACAUAAG-3′, respectively. siRNA against mouse *Tmem45b* was intrathecally injected via a chronic intrathecal catheter to KD *Tmem45b* in DRGs. Injections were given daily for 3 consecutive days.

Pain models. We used three pain models including an inflammatory pain model, a skin incision–induced tissue injury pain model, and a peripheral nerve injury–induced neuropathic pain model.

Behavioral tests. Behavioral responses to noxious heat and mechanical stimuli were assessed by applying a focused radiant heat source and calibrated von Frey filaments, respectively, to the plantar surface of the hind paw. Spontaneous pain-related behaviors were assessed by measuring the time spent flinching, biting, and licking. In addition, the CatWalk XT Version 10.6 (Noldus Information Technology, Wageningen, The Netherlands) was used for gait/locomotion analysis.

Retrograde labeling. DRG neurons innervating the hind paw skin, tibialis anterior muscle, distal colon, and urinary bladder were retrogradely labeled using Fast Blue (1% in PBS; Polysciences GmbH).

Immunohistochemistry and fluorescence in situ hybridization. We developed an antibody to mouse Tmem45b by immunizing a synthetic 264–278 amino acid peptide (GenBank #NM_144936.1). Digoxigenin-labeled cRNA probes were prepared to detect Tmem45b mRNA. Immunostaining, immunoelectron microscopy, and fluorescence in situ hybridization were performed in accordance with previous methods (31, 40, 55).

Western blot analysis. Western blot analysis was performed in accordance with previous methods (31).

qRT-PCR. All tissues were freshly isolated from adult C57BL/6N mice. The total RNA samples were extracted using the RNeasy Mini Kit (Qiagen). Experiments were carried out in triplicate using the LightCycler480 (Roche Diagnostic GmbH). For the analysis of mRNA expression in different tissues, *Gapdh* was used as a reference gene.

Gene profiling. RNA from DRG dissected from mice injected with IB4–saporin or saporin alone was isolated using an RNeasy Mini Kit (Qiagen). Amplified and biotinylated cRNA were then processed using an Affymetrix GeneChip Mouse Gene 2.0 ST Array, and signal values and detection calls (present or absent) for all transcripts were assigned using the GeneChip Command Console (TAC4.0; Affymetrix). Using the Robust Multiarray Average algorithm, Affymetrix CEL files were normalized for bioinformatics analysis.

Electrophysiology. Whole-cell patch clamp recordings were carried out as described in previous studies (56, 57). A 550-μm-thick transverse spinal cord slice attached to a dorsal root at the spinal level of L3–L5 was set in a chamber perfused with Krebs solution. Blind whole-cell voltage-clamp recordings were made from SG neurons.

Statistical analysis. Statistical analyses were performed in this study using JMP statistical software (version 14.2; SAS Institute, Cary, NC). We expressed quantitative data as the mean ± SD. For 2-group comparisons, statistics were based on the 2-sided paired or unpaired Student's *t* test, the Mann–Whitney rank-sum tests, or the χ^2 test. For multiple comparisons, 1-way ANOVA followed by Dunnett's test or 2-way ANOVA was performed unless indicated otherwise. P values < 0.05 were considered statistically significant.

Data, Materials, and Software Availability. All study data are included in the article and/or *SI Appendix*. The data is available upon reasonable request.

ACKNOWLEDGMENTS. We thank T. Ozasa at the Department of Immunology, Institute of Advanced Medicine, Wakayama Medical University School of Medicine for generating KO mice. We also thank D. Koga and T. Watanabe at Asahikawa Medical University for helpful discussion and technical assistance. This study was supported by grants from JSPS KAKENHI under grant numbers JP17H04322 (to T. Kawamata) and JP18K16460 (to T.T). We selected an open access license. We thank Melissa Crawford, PhD, from Edanz (https://jp.edanz.com/ac) for editing a draft of this manuscript.

Author affiliations: [a]Department of Anesthesiology, Wakayama Medical University School of Medicine, Wakayama 641-8509, Japan; [b]Department of Anatomy, Faculty of Medicine, Hokkaido University, Sapporo 063-8638, Japan; [c]Department of Immunology, Institute of Advanced Medicine, Wakayama Medical University School of Medicine, Wakayama 641-8509, Japan; and [d]Department of Neurophysiology, Hyogo College of Medicine, Nishinomiya 663-8501, Japan

1. C. J. Woolf, M. W. Salter, Neuronal plasticity: Increasing the gain in pain. *Science* **288**, 1765–1769 (2000).
2. J. Scholz, C. J. Woolf, Can we conquer pain? *Nat. Neurosci.* **5**, 1062–1067 (2002).
3. D. Julius, A. I. Basbaum, Molecular mechanisms of nociception. *Nature* **413**, 203–210 (2001).
4. A. I. Basbaum, D. M. Bautista, G. Scherrer, D. Julius, Cellular and molecular mechanisms of pain. *Cell* **139**, 267–284 (2009).
5. C. J. Woolf, Central sensitization: Implications for the diagnosis and treatment of pain. *Pain* **152**, S2–S15 (2011).
6. H. Kehlet, T. S. Jensen, C. J. Woolf, Persistent postsurgical pain: Risk factors and prevention. *Lancet* **367**, 1618–1625 (2006).
7. M. J. Caterina *et al.*, Impaired nociception and pain sensation in mice lacking the capsaicin receptor. *Science* **288**, 306–313 (2000).
8. R. K. Banik, T. J. Brennan, Trpv1 mediates spontaneous firing and heat sensitization of cutaneous primary afferents after plantar incision. *Pain* **141**, 41–51 (2009).
9. T. Hucho, J. D. Levine, Signaling pathways in sensitization: Toward a nociceptor cell biology. *Neuron* **55**, 365–376 (2007).
10. C. J. Woolf, Q. Ma, Nociceptors–noxious stimulus detectors. *Neuron* **55**, 353–364 (2007).
11. R. Z. Hill, D. M. Bautista, Getting in touch with mechanical pain mechanisms. *Trends Neurosci.* **43**, 311–325 (2020).
12. B. Lynn, S. P. Hunt, Afferent C-fibers: Physiological and biochemical correlations. *Trends Neurosci.* **7**, 186–188 (1984).
13. V. K. Shea, E. R. Perl, Sensory receptors with unmyelinated (C) fibers innervating the skin of the rabbit's ear. *J. Neurophysiol.* **54**, 491–501 (1985).
14. D. M. Cain, S. G. Khasabov, D. A. Simone, Response properties of mechanoreceptors and nociceptors in mouse glabrous skin: An in vivo study. *J. Neurophysiol.* **85**, 1561–1574 (2001).
15. C. Peirs, R. P. Seal, Neural circuits for pain: Recent advances and current views. *Science* **354**, 578–584 (2016).
16. D. J. Cavanaugh *et al.*, Distinct subsets of unmyelinated primary sensory fibers mediate behavioral responses to noxious thermal and mechanical stimuli. *Proc. Natl. Acad. Sci. U.S.A.* **106**, 9075–9080 (2009).
17. J. D. Silverman, L. Kruger, Selective neuronal glycoconjugate expression in sensory and autonomic ganglia: Relation of lectin reactivity to peptide and enzyme markers. *J. Neurocytol.* **19**, 789–801 (1990).

18. J. I. Nagy, S. P. Hunt, Fluoride-resistant acid phosphatase-containing neurones in dorsal root ganglia are separate from those containing substance P or somatostatin. *Neuroscience* **7**, 89–97 (1982).
19. D. C. Molliver *et al.*, IB4-binding DRG neurons switch from NGF to GDNF dependence in early postnatal life. *Neuron* **19**, 849–861 (1997).
20. D. C. Molliver, W. D. Snider, Nerve growth factor receptor TrkA is down-regulated during postnatal development by a subset of dorsal root ganglion neurons. *J. Comp. Neurol.* **381**, 428–438 (1997).
21. E. S. McCoy *et al.*, Peptidergic CGRPα primary sensory neurons encode heat and itch and tonically suppress sensitivity to cold. *Neuron* **78**, 138–151 (2013).
22. Y. Ye *et al.*, IB4(+) and TRPV1(+) sensory neurons mediate pain but not proliferation in a mouse model of squamous cell carcinoma. *Behav. Brain Funct.* **10**, 5 (2014).
23. L. G. Pinto *et al.*, Non-peptidergic nociceptive neurons are essential for mechanical inflammatory hypersensitivity in mice. *Mol. Neurobiol.* **56**, 5715–5728 (2019).
24. Y. Ye, D. Dang, C. T. Viet, J. C. Dolan, B. L. Schmidt, Analgesia targeting IB4-positive neurons in cancer-induced mechanical hypersensitivity. *J. Pain* **13**, 524–531 (2012).
25. K. Ono, Y. Ye, C. T. Viet, D. Dang, B. L. Schmidt, TRPV1 expression level in isolectin B_4-positive neurons contributes to mouse strain difference in cutaneous thermal nociceptive sensitivity. *J. Neurophysiol.* **113**, 3345–3355 (2015).
26. F. E. Holmes *et al.*, Transgenic overexpression of galanin in the dorsal root ganglia modulates pain-related behavior. *Proc. Natl. Acad. Sci. U.S.A.* **100**, 6180–6185 (2003).
27. S. K. Mishra, S. Holzman, M. A. Hoon, A nociceptive signaling role for neuromedin B. *J. Neurosci.* **32**, 8686–8695 (2012).
28. W. D. Snider, S. B. McMahon, Tackling pain at the source: New ideas about nociceptors. *Neuron* **20**, 629–632 (1998).
29. T. J. Price, C. M. Flores, Critical evaluation of the colocalization between calcitonin gene-related peptide, substance P, transient receptor potential vanilloid subfamily type 1 immunoreactivities, and isolectin B4 binding in primary afferent neurons of the rat and mouse. *J. Pain* **8**, 263–272 (2007).
30. J. W. Tarpley, M. G. Kohler, W. J. Martin, The behavioral and neuroanatomical effects of IB4-saporin treatment in rat models of nociceptive and neuropathic pain. *Brain Res.* **1029**, 65–76 (2004).
31. Y. Niiyama, T. Kawamata, J. Yamamoto, K. Omote, A. Namiki, Bone cancer increases transient receptor potential vanilloid subfamily 1 expression within distinct subpopulations of dorsal root ganglion neurons. *Neuroscience* **148**, 560–572 (2007).
32. M. Zwick *et al.*, Glial cell line-derived neurotrophic factor is a survival factor for isolectin B4-positive, but not vanilloid receptor 1-positive, neurons in the mouse. *J. Neurosci.* **22**, 4057–4065 (2002).
33. C. J. Woodbury *et al.*, Nociceptors lacking TRPV1 and TRPV2 have normal heat responses. *J. Neurosci.* **24**, 6410–6415 (2004).
34. H. Wang, M. J. Zylka, Mrgprd-expressing polymodal nociceptive neurons innervate most known classes of substantia gelatinosa neurons. *J. Neurosci.* **29**, 13202–13209 (2009).
35. B. Abrahamsen *et al.*, The cell and molecular basis of mechanical, cold, and inflammatory pain. *Science* **321**, 702–705 (2008).
36. A. M. W. Taylor, M. Osikowicz, A. Ribeiro-da-Silva, Consequences of the ablation of nonpeptidergic afferents in an animal model of trigeminal neuropathic pain. *Pain* **153**, 1311–1319 (2012).
37. D. I. MacDonald *et al.*, Silent cold-sensing neurons contribute to cold allodynia in neuropathic pain. *Brain* **144**, 1711–1726 (2021).
38. C. L. Li *et al.*, Somatosensory neuron types identified by high-coverage single-cell RNA-sequencing and functional heterogeneity. *Cell Res.* **26**, 83–102 (2016).
39. D. Usoskin *et al.*, Unbiased classification of sensory neuron types by large-scale single-cell RNA sequencing. *Nat. Neurosci.* **18**, 145–153 (2015).
40. K. Ishida, T. Kawamata, S. Tanaka, T. Shindo, M. Kawamata, Calcitonin gene-related peptide is involved in inflammatory pain but not in postoperative pain. *Anesthesiology* **121**, 1068–1079 (2014).
41. T. J. Brennan, P. K. Zahn, E. M. Pogatzki-Zahn, Mechanisms of incisional pain. *Anesthesiol. Clin. North America* **23**, 1–20 (2005).
42. S. Santana-Varela *et al.*, Tools for analysis and conditional deletion of subsets of sensory neurons. *Wellcome Open Res.* **6**, 250 (2021).
43. T. Wrzesiński *et al.*, Expression of pre-selected TMEMs with predicted ER localization as potential classifiers of ccRCC tumors. *BMC Cancer* **15**, 518 (2015).
44. S. Filipek, Molecular switches in GPCRs. *Curr. Opin. Struct. Biol.* **55**, 114–120 (2019).
45. K. Shen, W. Yu, Y. Yu, X. Liu, X. Cui, Knockdown of TMEM45B inhibits cell proliferation and invasion in gastric cancer. *Biomed. Pharmacother.* **104**, 576–581 (2018).
46. Y. Li *et al.*, Silencing transmembrane protein 45B (TNEM45B) inhibits proliferation, invasion, and tumorigenesis in osteosarcoma cells. *Oncol. Res.* **25**, 1021–1026 (2017).
47. R. Hu *et al.*, TMEM45B, up-regulated in human lung cancer, enhances tumorigenicity of lung cancer cells. *Tumour Biol.* **37**, 12181–12191 (2016).
48. L. C. Zhao *et al.*, TMEM45B promotes proliferation, invasion and migration and inhibits apoptosis in pancreatic cancer cells. *Mol. Biosyst.* **12**, 1860–1870 (2016).
49. R. P. Seal *et al.*, Injury-induced mechanical hypersensitivity requires C-low threshold mechanoreceptors. *Nature* **462**, 651–655 (2009).
50. D. Tavares-Ferreira *et al.*, Spatial transcriptomics of dorsal root ganglia identifies molecular signatures of human nociceptors. *Sci. Transl. Med.* **14**, eabj8186 (2022).
51. S. Gu *et al.*, Brain α7 nicotinic acetylcholine receptor assembly requires NACHO. *Neuron* **89**, 948–955 (2016).
52. E. J. Salm *et al.*, TMEM163 regulates ATP-gated P2X receptor and behavior. *Cell Rep.* **31**, 107704 (2020).
53. B. Duan *et al.*, Identification of spinal circuits transmitting and gating mechanical pain. *Cell* **159**, 1417–1432 (2014).
54. N. D. Volkow, F. S. C. Collins, The role of science in addressing the opioid crisis. *N. Engl. J. Med.* **377**, 391–394 (2017).
55. M. Yamasaki *et al.*, 3-Phosphoglycerate dehydrogenase, a key enzyme for l-serine biosynthesis, is preferentially expressed in the radial glia/astrocyte lineage and olfactory ensheathing glia in the mouse brain. *J. Neurosci.* **21**, 7691–7704 (2001).
56. S. C. Suzuki *et al.*, Cadherin-8 is required for the first relay synapses to receive functional inputs from primary sensory afferents for cold sensation. *J. Neurosci.* **27**, 3466–3476 (2007).
57. D. Uta *et al.*, TRPA1-expressing primary afferents synapse with a morphologically identified subclass of substantia gelatinosa neurons in the adult rat spinal cord. *Eur. J. Neurosci.* **31**, 1960–1973 (2010).